Magnetic K-edge absorption in $3d$ elements and its relation to local magnetic structure

S. Stähler and G. Schütz
Physik-Department E12, Technische Universität München, James-Franck-Strasse, D-8046 Garching, Germany

H. Ebert
Siemens AG, Central Research Laboratories, Paul-Gossen-Strasse 100, D-8520 Erlangen, Germany

(Received 20 April 1992)

In this paper we present a selection of circular magnetic x-ray dichroism (CMXD) measurements at the K edges of Fe, Ni, Co, and Mn in various alloys and compounds. We investigate the correlation between the measured spin-dependent absorption signal and the p-like spin polarization of the unoccupied bands at the Fermi level. In the case of Fe we find a direct correlation of the spin-dependent absorption profile to the p-like spin polarizations. This is discussed for various alloys. The measured CMXD signals are compared with theoretical calculations for the absorption spectra. For Fe and Ni we have performed spin-polarized relativistic Korringa-Kohn-Rostoker Green's function calculations, which give a parameter-free description of the spin-dependent absorption process. The content of information in the experimental CMXD spectra on the local magnetic p and d moments is discussed in comparison with the calculated changes of the p and d moments. In the case of the Co and Ni K edges we find a direct correlation of the average strength of the spin-dependent absorption signal to the p moment. For Co also a direct correlation to the d moment is indicated. At Fe K edges no proportionality of any features of the spin-dependent absorption profile to p or d moments have been found.

I. INTRODUCTION

During the last years, a variety of methods which use synchrotron radiation of well-defined polarization in the x-ray energy range have been developed to address magnetic aspects in the electronic structure of condensed matter.[1–6] One of these kinds of approaches is the spin-dependent absorption spectroscopy probing circular magnetic x-ray dichroism (CMXD). The existence of CMXD was convincingly demonstrated at the K edge of Fe,[3] and at the L edges of $4f$ atoms[7] and heavier $5d$ impurities in Fe.[8] Recently, also in the soft-x-ray energy range, the corresponding dichroic effects at the $L_{2,3}$ edges of $3d$ elements and the $M_{4,5}$ edges of $4f$ elements have been studied.[6]

In $3d$ ferromagnetic systems, the measurement of spin-dependent absorption at the $L_{2,3}$ edges is a promising method to investigate the polarization characteristics of $3d$ states, which are mainly responsible for the magnetism. Because of the strong absorption in the corresponding regime of the radiation energy, the absorption coefficient μ has to be determined indirectly in this case via electron or fluorescence detection. However, the former can be difficult in the vicinity of magnetic fields, while the latter is restricted to dilute systems and thin layers because of autoabsorption effects. Though the CMXD at the K edges is more than one order of magnitude smaller than at the L edges, it might nevertheless provide interesting information on the magnetic properties of the investigated system. Furthermore, measurements at the K edge have—compared to the $L_{2,3}$ edges—the great advantage that they do not require UHV vacuum conditions, because of the high excitation energies of more than 6 keV for heavier $3d$ elements. This feature allows a very easy handling and changing of the samples.

The high penetration power of hard x-rays allows bulk-sensitive measurements not being influenced by surface effects. In many systems the very accurate transmission method can be applied, and additionally in a large variety of powder and polycrystalline samples, the transmitted intensity can be used as incident intensity for a reference absorber, thus detecting small differences of the absorption profiles in the second absorber of a linear three-chamber arrangement.

The quantities determined in a CMXD experiment are the absorption coefficients μ^+ and μ^- for circularly polarized x-rays incident with spin antiparallel $(+)$ and parallel $(-)$, respectively, to the magnetization direction of the target, i.e., parallel and antiparallel to the spins of the majority like electrons in the ferromagnetic (ferrimagnetic) absorber. The normalized spin-dependent absorption profile $\mu_c/\mu_0=(\mu^+-\mu^-)/(\mu^++\mu^-)$ is thickness independent and a "fingerprint" of the magnetic properties of the system. It is as characteristic for the local magnetic properties of the absorbing atomic species as the conventional absorption profile μ_0 itself, which reflects global electronic properties. At the K edges of $3d$ transition metals, μ_0 is related to the density of final states of p symmetry because of the dipole selection rules implying transitions from the $1s$ core state to the $4p$ conduction band. The contribution of quadrupole transitions $(1s\rightarrow 3d)$ is expected to be more than two magnitudes smaller with respect to the dipole part[9] and can be neglected in case of metallic samples.[10]

The occurrence of spin-dependent absorption originates in the spin polarization of the empty electronic states and the presence of spin-orbit coupling. In some

cases such as, e.g., at the $L_{2,3}$ edges of $5d$ impurities in Fe, it could be shown that the $\mu_c/\mu_0(E)$ spectra are nearly proportional to the relative spin polarization $\Delta\rho/\rho=(\rho^+-\rho^-)/(\rho^++\rho^-)$ of the final empty states, i.e., the relative difference in the density of states with parallel (ρ^+) and antiparallel (ρ^-) alignment of the electron spin with respect to the majority d electrons. Relying on this relationship, the experimental CMXD spectra can be used to deduce estimates of the local magnetic moments.[11]

As shown below, the correlation between the spin-dependent absorption at the K edges and the spin polarization of the final p states is much more complicated. Nevertheless, it was found that the changes in the amplitudes of the μ_c/μ_0 spectra at the K edges are intimately related to the changes of the local spin polarization of the absorbing atom, which therefore can be studied as a function of external parameters such as, e.g., the temperature, external magnetic field, and pressure.

Although the measurements of the spin-dependent K absorption do not lead to direct information on the local magnetic moments which are predominantly carried by d electrons, it is demonstrated in the following that in case of Co and Ni there exists a clear correlation between the spin-dependent absorption signal and the p moments. Apart from this we present a number of further applications of spin-dependent K absorption to study magnetic $3d$ systems.

In Sec. II the experimental technique is presented that allows us to determine the CMXD signal with high accuracy. Our theoretical model, which interprets the spin-dependent absorption profile directly in terms of the p-like spin polarization, is discussed in Sec. III A. To prove the interpretation of our experimental data on the basis of this model, we have performed rigorous calculations of the absorption spectra. The essential features of this approach are summarized in Sec. III B. In Sec. IV the experimental data for the K edges of Fe, Co, Ni, and Mn in various compounds, alloys, and multilayered structures are presented. In Sec. V the experimental spectra are related to the local spin polarization using our model in comparison with the results of our spin-polarized band-structure calculations. In contrast to this, our calculated CMXD spectra can be confronted directly with the experimental data without using any assumption in analyzing these data. The relationship of the spin-dependent K absorption and the local magnetic moments are discussed by a comparison of our calculated p and d moments with the strengths of the CMXD signal for various systems.

II. EXPERIMENTAL SETUP AND DATA ANALYSIS

All the measurements presented were performed at the Hamburger Synchrotron Strahlungslabor HASYLAB at the electron storage rings DORIS II and DORIS III. The principle of the setup for the highly precise transmission measurements at a distance of 28 m from the photon source point is shown in Fig. 1.

The incident photons pass a vertically adjustable double slit, which is fixed to a double-ionization chamber I_w so that two beams symmetrically to the electron orbit pass with opposite sense of circular polarization. In the correct position, the intensities of the two beams have to be equal, yielding to equal counting rates in the upper and lower ionization chamber of I_w. A typical degree of circular polarization P_c of the white beam,[12] which can be achieved with this arrangement, is $P_c=\pm 0.8$ if the double slit is adjusted properly. The photons are monochromatized using Si(111) reflections in a double-crystal spectrometer, providing an energy resolution of $\Delta E_\gamma/E_\gamma \sim 4\times 10^{-4}$.

The quality of the polycrystalline samples was checked by x-ray-diffraction measurements. The targets were placed inside a water-cooled solenoid, producing a mag-

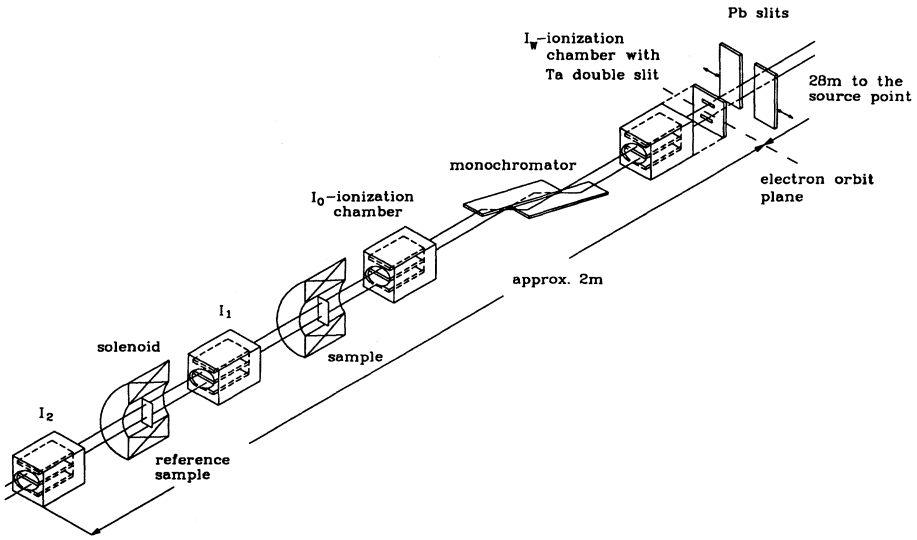

FIG. 1. Principle of the experimental setup for measurements in the transmission mode using the double-ionization chamber arrangement. For further details, see text.

netic field of up to 0.2 T with its direction (anti)parallel to the photon propagation direction. The sign of the magnetic field was flipped every second The absorption measurements were carried out measuring the incident and transmitted intensities I_0 and I_1 by double-ionization chambers. The two transmitted beams with opposite degrees of circular polarization were measured simultaneously and independently of each other, thus reducing systematic errors. A third double-ionization chamber (I_2) was placed behind the second target, enabling measurements with the reference sample. With this setup it was possible to study the magnetic absorption of one element simultaneously in two distinct chemical environments, thus minimizing the influence of possible instabilities in the degree of the polarization of the synchrotron radiation. This allows the detection of small energy shifts in the absorption spectra and the quantitative determination of differences in the amplitude and structure of the spin-dependent absorption profile between the sample and the well-known reference sample. Such differences can also be examined with respect to their dependence on external parameters such as, e.g., temperature and magnetization.

The measured intensities in our experiment are related by the simple expression

$$I^{\pm}(E)=I_0^{\pm}(E)e^{-\mu^{\pm}(E)d} ,$$

where d is the sample thickness and μ the absorption coefficient. The $+$ and $-$ signs denote antiparallel and parallel alignment, respectively, of the spins of the circularly polarized photons and macroscopic magnetization. The absorption coefficient $\mu^{\pm}$ can be split into a spin-dependent part (μ_c) and a spin-independent part (μ_0):

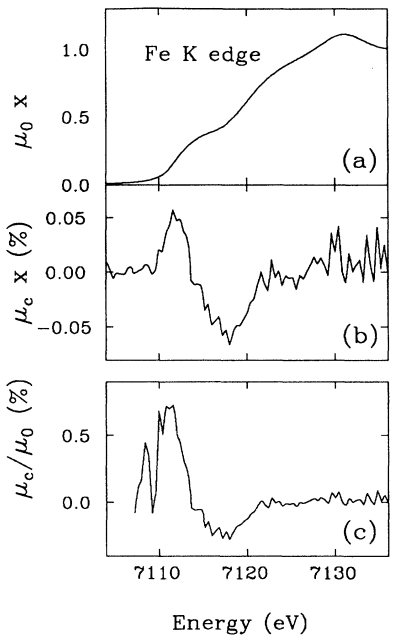

FIG. 2. Typical single spectra for $\mu_0 x$ (top), $\mu_c x$ (middle), and μ_c/μ_0 spectra (bottom) at the K edge of Fe metal.

$$\mu^{\pm}(E)=\mu_0(E)\pm\mu_c(E) ,$$

$$\mu_0 d=\tfrac{1}{2}(\ln I_0^{+}/I^{+}+\ln I_0^{-}/I^{-}) ,$$

$$\mu_c d=\tfrac{1}{2}(\ln I_0^{+}/I^{+}-\ln I_0^{-}/I^{-}) .$$

Typical $\mu_0 d$ and $\mu_c d$ spectra for Fe metal can be seen in Figs. 2(a) and 2(b). To get rid of the background in the pre-edge region, the absorption in an energy region of 100 eV before the edge was measured very carefully. So it was possible to fit the background with a Victoreen function $f=C\lambda^3-D\lambda^4$,[13] where λ is the x-ray wavelength and C,D are free parameters, and substract it from the absorption spectra.

In order to get a thickness-independent signal, the spin-dependent absorption coefficient μ_c is divided by μ_0 [see Fig. 2(c)]. Because of the division by the very small absorption coefficient dropping to zero in the pre-edge region, this procedure gives rise to rather large error bars in the vicinity of the absorption edge for the presented spectra. In a typical measurement time of about 2 h an accuracy of μ_c/μ_0 of better than 10^{-4} can be achieved whereby up to ten single spectra with energy steps of 0.2 eV were accumulated. The near-edge part of a typical Fe-metal single spectrum taken within 10 min is presented in Fig. 2. Figure 2(a) shows $\mu_0 x$, Fig. 2(b) $\mu_c x$, and Fig. 2(c) μ_c/μ_0.

III. THEORETICAL ASPECTS

A. Simple model for the interpretation of CMXD spectra

To find a relation between the spin-dependent absorption profile $[\mu_c/\mu_0](E)$ and the spin polarization $[\Delta\rho/\rho](E)$ of the unoccupied states above the Fermi level, a simple "two-step" model based on the single-particle band-structure approximation can be used. According to Fermi's golden rule, the absorption coefficient $\mu(E)\sim|M|^2\rho(E)$ is related to the transition matrix element M and the density of final states which can be populated according to the dipole selection rules. Since M and its energy dependence are not easy to determine, it is desirable to find a description which does not involve M. Applying Fermi's golden rule to the spin-resolved absorption channels permits one to write, approximately,

$$[\mu_c/\mu_0](E)=P_e[\Delta\rho/\rho](E) , \quad (1)$$

where the proportionality factor P_e can be understood as a photoelectron spin polarization, i.e., the expectation value of the photoelectron spin in the direction of the photon k vector. It results in analogy to the Fano effect in the optical energy range[14] from the conservation of the angular momentum in the absorption process together with the spin-orbit coupling acting on the initial and/or final states. To estimate P_e in the case of K absorption, one looks at a free atom absorbing a right circularly polarized photon, which results in a change of the orbital quantum number m_l of the photoelectron of $\Delta m_l=+1$. In case of the $p_{1/2}$ final state, only the transition

$$|m_l=0,\ \sigma=-1\rangle\rightarrow|m_l=+1\ ,\ \sigma=-1\rangle \quad (A)$$

is allowed. In case of a $p_{3/2}$ final state, two transitions

$$|m_l=0\ ,\ \sigma=-1\rangle \rightarrow |m_l=+1\ ,\ \sigma=-1\rangle\ (B_1)$$

and

$$|m_l=0\ ,\ \sigma=+1\rangle \rightarrow |m_l=+1\ ,\ \sigma=+1\rangle\ (B_2)$$

are possible. In the experiment a separation of the channels A, B_1, and B_2 is not possible. In case of nonrelativistic quantum mechanics, the transition probabilities are $W_A=\frac{1}{4}$, $W_{B1}=\frac{1}{8}$, and $W_{B2}=\frac{3}{8}$, resulting in an average value of

$$P_e=\frac{\sum_{i,f}\langle\sigma\rangle_f W_{\rm if}}{\sum_{i,f}W_{\rm if}}=0\ . \tag{2}$$

Since in the initial s state no spin-orbit splitting is present, only the spin-orbit interaction in the final states must be considered, resulting in small deviations of the transition probabilities W from the nonrelativistic value and therefore to nonvanishing photoelectron polarization of the order of $|P_e|\sim 10^{-2}$. Unfortunately, in calculating P_e along these lines using modified atomic codes, it turns out that the results depend very sensitively on the details of the calculation. Using the code of Ref. 15, we have calculated for a free Fe (Ni) atom a value of $P_e=-0.3\%$ (-0.4%), while using the dipole matrix elements of Ref. 16 one finds rather different values of $P_e\sim+0.8\%$ ($+0.9\%$) of opposite sign. Furthermore, on using the above relationship between μ_c/μ_0 and $\Delta\rho/\rho$, we ignore any energy dependence of P_e. We also want to note that, because of the constraint $\Delta m_l=1$, the photoelectron has a large expectation value of the orbital angular momentum of $\langle l_z\rangle=1$, and thus the existence of a nonvanishing angular momentum, which has been neglected in this model, will also influence the CMXD signal. In contrast to this, such problems do not arise in calculating the absorption coefficient by the method described below.

B. Calculation of the absorption spectra

The absorption coefficient μ can be viewed as a direct measure for the quantum-mechanical transition probabilities $W_i^{q\lambda}$ summed for the excitation of reachable core states i by radiation of the wave vector $\mathbf{q}$ and polarization λ:

$$\mu(E)\sim\sum_i W_i^{q\lambda}\ . \tag{3}$$

A very general formalism to study excitation processes of this type has been given by Durham.[17] Within this framework, $W_i^{q\lambda}$ for transitions of a core electron in a state Φ_i into the conduction band is given by

$$W_i^{q\lambda}=-\frac{1}{\Gamma}\int d^3r\,d^3r'\,\Phi_i^*(\mathbf{r})X_{q\lambda}(\mathbf{r})\times{\rm Im}G^+(\mathbf{r},\mathbf{r}',E_i+\hbar\omega)X_{q\lambda}^*(\mathbf{r}')\Phi_i(\mathbf{r}')\times\Theta(E_i+\hbar\omega-E_F)\ , \tag{4}$$

where Θ is the step function.

As is clear from the remarks made above, a description of the CMXD has to take spin polarization as well as spin-orbit coupling into account.[9] This can be done rigorously by using Eq. (4) in its relativistic form. The corresponding electron-photon interaction operator $X_{q\lambda}(\mathbf{r})$ is given by

$$X_{q\lambda}(\mathbf{r})=-e\boldsymbol{\alpha}\cdot\mathbf{A}(\mathbf{r})\ , \tag{5}$$

where $\boldsymbol{\alpha}$ is the Dirac matrix vector and $\mathbf{A}(\mathbf{r})$ is the vector potential due to the photon field. A very powerful formulation for the Green's function $G^+(\mathbf{r},\mathbf{r}',E)$, which represents the manifold of final states in the unoccupied part of the conduction band, is provided by the spin-polarized version of relativistic multiple-scattering theory [spin-polarized relativistic Korringa-Kohn-Rostoker Green's function (SPR-KKR-GF)].[18] Accordingly, the imaginary part of $G^+(\mathbf{r},\mathbf{r}',E)$ can be written as

$${\rm Im}G^+(\mathbf{r},\mathbf{r}',E)=\sum_{\Lambda\Lambda'}Z_\Lambda(\mathbf{r},E){\rm Im}\tau_{\Lambda\Lambda'}(E)Z_{\Lambda'}^\dagger(\mathbf{r}',E)\ . \tag{6}$$

Here the index Λ represents the set of relativistic quantum numbers (κ,μ) and the functions $Z_\Lambda(\mathbf{r},E)$ are the scattering solutions to the single-site Dirac equation for a spin-dependent potential.

The above expression for the Green's function by means of the site-diagonal scattering path operator $\tau_{\Lambda\Lambda'}^{nn}(E)$ provides an extraordinary flexibility to the adopted approach, which allows it to be applied to pure systems,[9,19] impurity systems,[11] or even disordered alloys.[20] According to the specific situation, one merely has to insert into Eq. (6) the component-projected scattering path operator $\tau_{\Lambda\Lambda'}^{nn\alpha}(E)$ and the wave functions $Z_\Lambda^\alpha(\mathbf{r},E)$ calculated for the potential of the component α. For disordered alloys this is done within the framework of the coherent potential alloy theory.[20]

To compare the theoretical spectra resulting from an application of Eq. (4) with experiment, we have taken the various relevant broadening mechanisms—intrinsic and apparative—into account in a way similar to that described by Müller, Jepsen, and Wilkins.[21]

IV. RESULTS

Comparing the K-edge absorption-spectra in the different iron bcc compounds (Fig. 3), one finds a nearly identical shape of the polarization-averaged absorption spectra, which is typical for bcc structure. This behavior—although to much less degree—is also found for the spin-dependent absorption profiles which show a prominent maximum at $E=0$ eV followed by a minimum located at about 5 eV. Besides this similarity also some significant differences have been found. In $Fe_{80}Co_{20}$ the first peak at 0 eV is reduced whereas the negative minimum is increased. By adding Pt to Fe metal, a significant peak with positive sign appears at 8 eV. As for the fcc systems studied, for both investigated fcc alloys a K-edge absorption spectrum typical for the fcc structure has been found. Comparing the results for two Pt concentrations, one finds small differences in the shape of the absorption edge. The CMXD spectra of these alloys are identical within the statistical accuracy. The mean values of these spin-dependent spectra are more positive than the signal in bcc samples. Additional differences are the two pronounced minima in the upper

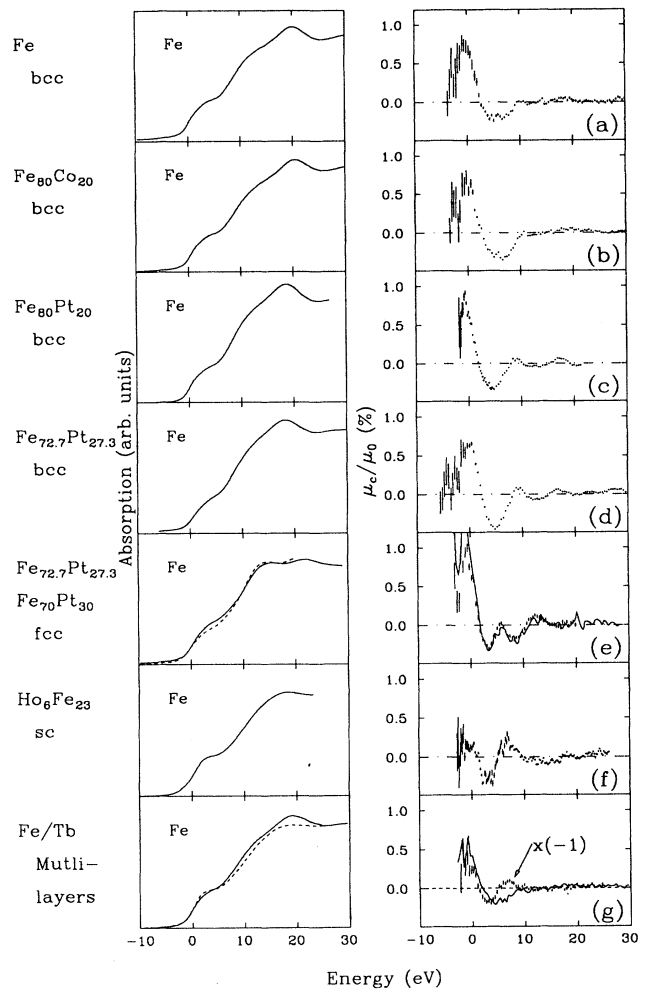

FIG. 3. Spin-integrated (left) and spin-dependent (right) absorption spectra at the Fe K edges of (a) Fe metal, (b) $Fe_{80}Co_{20}$, (c) $Fe_{80}Pt_{20}$, (d) bcc $Fe_{72.7}Pt_{27.3}$, (e) fcc $Fe_{72.7}Pt_{27.3}$ (dashed line) and $Fe_{70}Pt_{30}$ (solid line), (f) Ho_6Fe_{23}, and (g) 4 nm Fe/0.7 nm Tb (solid line) and 1 nm Fe/2.6 nm Tb (dashed line).

energy range. The Fe K edge in Ho_6Fe_{23} shows an absorption-edge profile typical for binary $3d$-$4f$ compounds. The shape of the CMXD spectra is rather different compared to the metal and alloys because of the absence of a strong negative peak at the absorption threshold and the significant maximum appearing at 7 eV. The results of Fe/Tb multilayered structures with small (1 nm Fe/4 nm Tb) (dashed line) and large content of Fe (4 nm Fe/0.7 nm Tb) (solid line) are shown in Fig. 3(g). The angle θ between the magnetization direction of the target and incident photons was chosen as 0° for the former sample, because the easy-magnetization axis is perpendicular to the surface. The latter sample was measured under 30° because of the in-plane easy-magnetization direction. The absorption spectrum of the (4 nm Fe/0.7 nm Tb) structure looks very much like bcc Fe, while the μ_c/μ_0 signal shows—within the statistical accuracy—a spectrum which is like the Fe-metal spectrum, but with decreased amplitude. This is attributed to

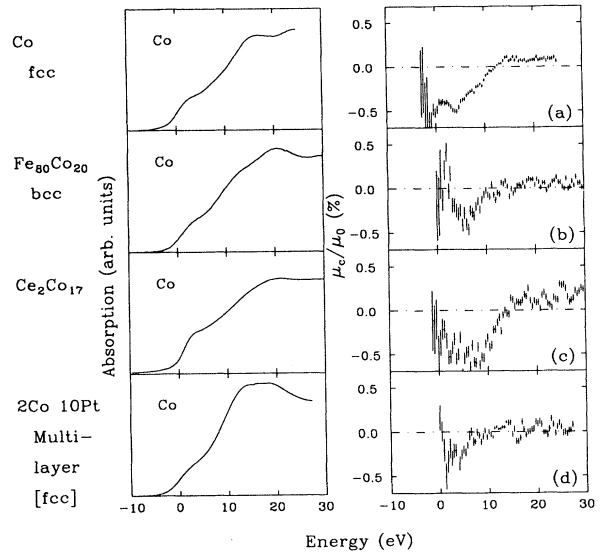

FIG. 4. Spin-integrated (left) and spin-dependent (right) absorption spectra at the Co K edges of (a) Co metal, (b) $Fe_{80}Co_{20}$, (c) Ce_2Co_{17}, (d) Co/Pt multilayer.

a not complete sample magnetization under the experimental conditions. The polarization-averaged absorption spectrum in the (1 nm Fe/4 nm Tb) sample resembles neither the fcc nor bcc structured Fe-based alloys, but shows obviously similarity with that of Ho_6Fe_{23}. The corresponding μ_c/μ_0 signal shows an assimilation between the intermetallic compound Ho_6Fe_{23} and Fe metal. The signal of sample 1 is plotted with a reversed sign to make it easier for the eye to compare the shape of the spectra. Note that the Fe/Tb multilayers are not normalized to 100% magnetization.

Considering the normal Co absorption spectra in Fig. 4, the Co metal has a typical fcc[22] absorption profile which is very similar to the Fe alloys with fcc structure, while the $Fe_{80}Co_{20}$ alloy has a typical bcc structure. Ce_2Co_{17} shows a shoulder around 0 eV as it can often be found in intermetallic compounds such as Ho_6Fe_{23} and Fe/Tb multilayers with a large part of Tb. The spectrum of the 4 Å Co/23 Å Pt multilayered sample grown in fcc structure[23] (measured in $\theta=0°$ geometry) is significantly different from the pure Co. The spin-dependent absorption profiles at the Co K edge are mainly negative, whereas they evidently differ from the spectra at the Fe K edge. Only at the Co K edge of the $Fe_{80}Co_{20}$ alloy is the existence of a low-lying positive peak indicated. The negative signal in the energy range of about 0–10 eV is max-

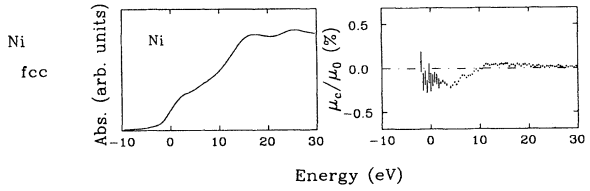

FIG. 5. Spin-integrated (left) and spin-dependent (right) absorption spectra at the Ni K edge in Ni metal.

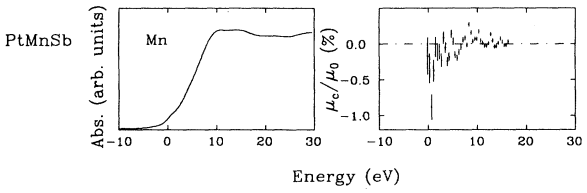

FIG. 6. Spin-integrated (left) and spin-dependent (right) absorption spectra at the Mn K edge in PtMnSb.

imum in Co metal and reduced by 50% in the Co/Pt multilayer. The Co/Pt multilayer also shows a narrowing and a reduction of the CMXD signal, while in the Ce_2Co_{17} compound it is more broadened, resulting in a larger average amplitude compared to the metal.

The normal Ni K absorption profile (Fig. 5) looks like a typical fcc compound. The spin-dependent absorption profile in Ni is negative, but becomes slightly positive above 10 eV and resembles the shape of the Co spectrum with a reduced amplitude by a factor 0.3–0.4.

The Mn K edge in $Pt_xMn_{1-x}Sb$ (Fig. 6) has a very steep absorption edge with the small indication of a step at around 0 eV. The CMXD spectrum shows a narrow negative peak with strong statistical inaccuracy in the energy region of the prepeak.

V. DISCUSSION

In a first step, we check whether, based on the simplified model described in Sec. III A, a direct correlation between the spin-dependent K absorption signal and the p-like spin densities exists. In the left-hand part of Fig. 7, it is demonstrated that in case of iron and nickel metal the structures of the polarization-averaged K absorption profile can be related to the p-projected density of states above the Fermi level (broadened by 1 eV Lorentzian). The corresponding p-like spin polarizations $\Delta\rho/\rho$ (dashed line), which result from spin-polarized relativistic Korringa-Kohn-Rostoker Greens'-function SPR-KKR-GF calculations, ar shown in the right-hand panel. The theoretical $\Delta\rho/\rho$ spectra were broadened with a Lorentzian line of 1 eV width and a Gaussian line of 3 eV width to account for the finite lifetime of the core hole and for experimental broadening, respectively. The experimental broadening is due to the monochromator crystal which causes an energy-dependent broadening of $\Delta E = \cot\alpha_{\text{Bragg}}\Delta\theta E$, where α_{Bragg} is the Bragg angle and $\Delta\theta$ takes into account the beam divergence and Rocking curve width of the used crystal. An estimate for the electron polarization parameter P_e can be obtained by comparing this curve with the experimental μ_c/μ_0 spectrum. Here one should note that it is, in principle, unknown which energy point of the experimental spectra corresponds exactly to the Fermi level. But the direct correlation between the density of states and the bumps in the absorption edges identifies the origin of the experimental energy scale as the Fermi level. For this reason the first positive peak of the μ_c/μ_0 spectrum can, besides a shift of 3 eV, be correlated to a positive spin polarization of the unoccupied states at E_F. From Fig. 7 one deduces, for Fe, $P_e \sim +3\%$. This agrees in sign with the result from our atomic-type calculations ($+0.8\%$) using matrix elements from Ref. 16, but is much higher in magnitude. For Ni the sign of P_e is negative and in the order of -2%. This is again much higher than the results for P_e of -0.4% calculated using the modified atomic code of Ref. 15. These results demonstrate that, although the spin splitting of the final p-projected states accounts for the spin dependence at the K edges, the correlation between the experimental μ_c/μ_0 spectra and $\Delta\rho/\rho$ can differ strongly within the $3d$ row. Obviously, it depends extremely on the details of the band structure, resulting in a significant energy dependence of the proportionality factor P_e. Therefore the correlation between the CMXD profile and the final-state spin density cannot be deduced from atomic calculation of the dipole matrix elements giving constant values for P_e, which on the other hand are very sensitive on the details of the computations.

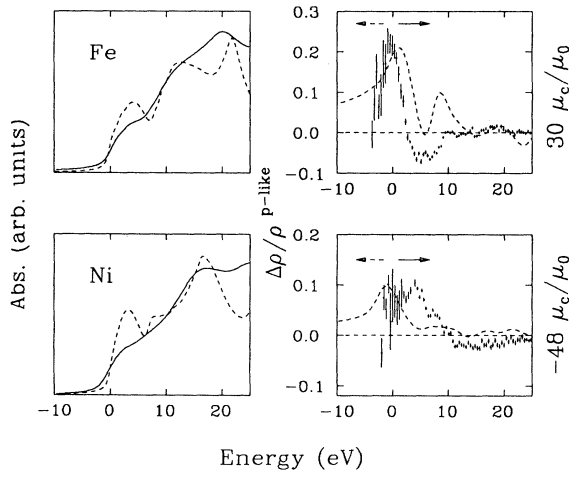

FIG. 7. Experimental spin-integrated absorption profile and theoretical (dashed line) p-projected density of states above the Fermi level are compared in the case of Fe and Ni metals. The right-hand part shows the theoretical spin density (dashed line, left-hand scale) and the spin density deduced from the μ_c/μ_0 signal (right-hand scale) rescaled by a factor of 30 for Fe and by a factor of -48 for Ni.

A possible origin of this behavior is the nonvanishing angular momentum in the final p states, which is possibly not completely quenched as has been found for the d states. Looking at the ratio $\mu_{\text{Bahn}}/\mu_{\text{spin}}$, one finds $\mu_{\text{Bahn}}/\mu_{\text{spin}} = 0.09/2.2 = 0.04$ for Fe and $\mu_{\text{Bahn}}/\mu_{\text{spin}} = 0.07/0.7 = 0.1$ for Ni, showing that the contribution of the angular momentum in Fe is smaller than in Ni. This can be the reason why the simple picture gives a better agreement of the theoretical and experimental spin densities in the case of Fe than for Ni. The existence of an angular momentum in the p-like final states can have a significant contribution even if the angular momentum is very small, as a result of the expectation value of the photon angular momentum, which is $\langle l_z \rangle = 1$.

The next step of the interpretation is the comparison of the experimental findings with the fully relativistic SPR-

KKR-GF calculations for the absorption of circularly polarized light in ferromagnets. It can be seen from a comparison of the measured and calculated absorption profiles (Fig. 8, left-hand panel) that the structure, i.e., the position of the peaks, is fairly well described by theory, but that the experimental spectra seem to be somewhat broader. Comparing the theoretical μ_c/μ_0 spectra with the experimental data (Fig. 8, right-hand panel), one finds up to 4 eV a much better quantitative and qualitative agreement in case of Fe as is found by a direct comparison with the p-projected spin density. This again underlines the importance of including the matrix element properly. Some differences are found at 11 eV where theory predicts a positive peak of $+0.25\%$, while the experimental CMXD signal drops to zero. Although in the case of Ni the agreement is not as good as in Fe, especially in the higher-energy range, the theoretical spectrum describes well the negative sign and magnitude of the experimental signal. The agreement shows that our theoretical formalism allows a parameter-free description of the experimental findings. However, comparing the calculated μ_c/μ_0 spectra with the calculated $\Delta\rho/\rho$ spectra, it is obvious that like the simplified model the calculation of the CMXD signal finds a correlation between them, since it is predicted that the positive peak in the spin density at 9 eV is correlated to a positive peak in the μ_c/μ_0 spectra in disagreement with the experimental data.

In the case of the remaining CMXD spectra, our systematic studies indicate that, although the correlation of the spin-dependent absorption and spin structure of the p bands is very complex, we can get useful information on the magnetic aspects of the electronic structure by spin-dependent K absorption: Looking at the μ_c/μ_0 spectra (Figs. 3 and 4) and the Fe K edge in Fe metal and $Fe_{80}Co_{20}$ and at the Co K edge in Co metal, one finds that the $Fe_{80}Co_{20}$ spectrum becomes more negative compared to Fe; i.e., it shows an assimilation of the spin-dependent absorption profile of Fe to the one of Co. Similar behavior has been observed in Fe-Ni alloys.[24] This is according to the expected assimilation of the spin polarization, since both components have a more or less common s-p band. This shows that the variation of the local spin structure by alloying different d elements is directly manifested in the CMXD signal. By adding Pt to Fe metal (Fig. 3), a change of the spin structure is also reflected by the CMXD signal. A positive peak at 8 eV, which is theoretically predicted for Fe metal, is clearly visible for bcc $Fe_{80}Pt_{20}$ and is even more pronounced in bcc $Fe_{72.7}Pt_{27.3}$; i.e., the peak is growing with growing Pt concentration, and the amplitude of the minimum increases and resembles even more the theoretical Fe spectra. This might be a hint to an additional spin splitting at 7 eV. In the case of the martensitic transition from bcc to fcc in $Fe_{72.7}Pt_{27.3}$, the experimental finding indicates that the positive spin polarization at the Fermi level increases by 30% correlated with the unoccupied p band at the Fermi level becoming more positive. At the higher energies, a drastic change of spin polarization between fcc and bcc structures is observed. The motivation to investigate these Fe/Pt alloys was their Invar behavior; i.e., the thermal expansion coefficient as a function of temperature is almost constant in a broad range around room temperature.[25] This phenomenon results from a complex interrelationship of lattice expansion and the magnetic properties of the system due to spin fluctuations. Changing the magnetic properties of the Invar alloy, i.e., adding more Pt to $Fe_{72.7}Pt_{27.3}$ to get $Fe_{70}Pt_{30}$, changes the lattice constant by $+0.2-0.3\,\%$.[26] As seen from the normal absorption profile this leads to an decrease of ρ at around 5 eV. In contrast to this, the *spin-dependent* absorption data indicate that this is *not* correlated to a change in the relative spin density, which is possibly a typical behavior for Invar alloys.

In the Fe/Tb multilayered samples, the signal of the sample with the larger amount of Fe is very close to the Fe metal, but with somewhat reduced amplitude at the prominent maximum. Going to the composition Fe(10 Å)/Tb(26 Å), this positive peak at the Fermi level decreases whereas an increase of the spin splitting at higher energies as is found in the cubic binary compound Ho_6Fe_{23}. In Ho_6Fe_{23} the CMXD signal at $E=0$ eV is collapsed, whereas the maximum at 7 eV becomes very strong, indicating that here the spin splitting of the p-like density at the Fermi level is significantly reduced while the unoccupied p-like density rises at about 7 eV. We interpret the assimilation of the CMXD in Fe(10 Å)/Tb(26 Å) to the spectra of the complex compound Ho_6Fe_{23} by a significant formation of intermetallic compounds or alloys in the interlayer region. This finding is confirmed by our CMXD studies at the Tb $L_{2,3}$ edges[27] and Mössbauer measurements.[28] This demonstrates that from the CMXD spectra one can get information on the chemical structure of the sample, which is important for the understanding of macroscopic magnetic properties, especially for multilayered structures.

An extra-ordinary case concerning the structure of the CMXD signal is the Mn K edge in $Pt_xMn_{1-x}Sb$. By interpreting the spectra in terms of spin densities similar as

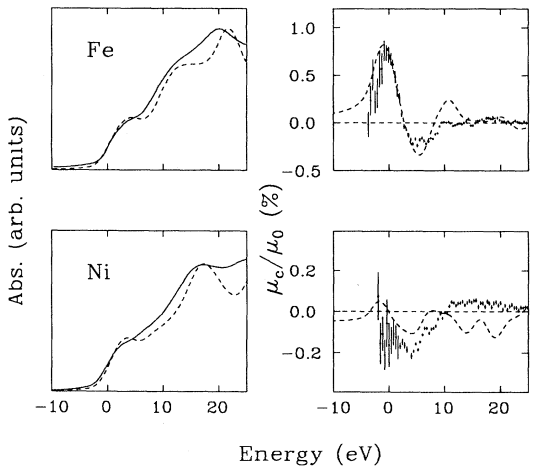

FIG. 8. Experimental and theoretical (dashed line) spectra for the spin-integrated absorption (left) and spin-dependent absorption (right) are compared in the case of Fe and Ni metals.

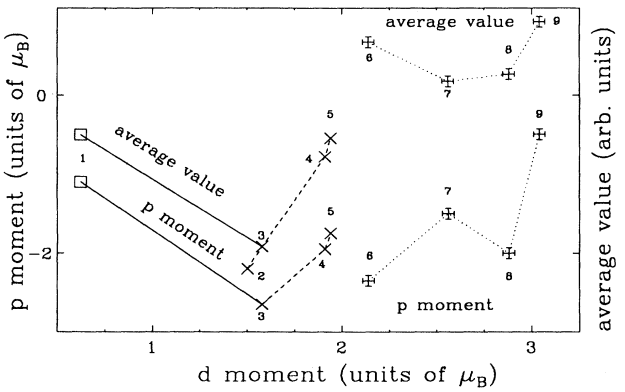

FIG. 9. Theoretical p moment and average value of the μ_c/μ_0 signal plotted vs the theoretical d moment for various compounds: (1) Ni K edge in Ni metal, (2) Co K edge in Ce_2Co_{17}, (3) Co K edge in Co metal, (4) Co K edge in $Fe_{80}Co_{20}$, (5) Co K edge in Pt/Co multilayered structure, (6) Fe K edge in Fe metal, (7) Fe K edge in $Fe_{80}Co_{20}$ bcc, (8) Fe K edge in $Fe_{72.7}Pt_{27.3}$ bcc, and (9) Fe K edge in $Fe_{72.7}Pt_{27.3}$ fcc.

in iron, the results are a hint for a very large spin density at the Fermi level. This confirms the theoretical expectation that $Pt_xMn_{1-x}Sb$ is a half-metallic ferromagnet[29] where, because of the band gap for the minority-spin subsystem, the final states at the Fermi level are completely polarized.

A. Correlation between the CMXD signal and local magnetic moments

From the Fe results as well as from the results of the alloys, where the spin-dependent spectra are dominated by the prominent peak at 0 eV, one might tend to conclude that this feature is typical for Fe and can be used to determine the orientation of the Fe atom in complicated systems. But that this is not the case or should be handled with care show our results of Ho_6Fe_{23}, where the Fe moment has nearly the same value as in Fe metal,[30] but exhibits no prominent maximum at $E=0$ eV. That the iron CMXD signal cannot easily be related to the local moments is confirmed by our calculations of the variation of the p and d moments in various systems. To compare these results with the experimental data, we have taken as a measure for the μ_c/μ_0 signal the average value between -2 and 22 eV. In Fig. 9 we show the theoretical p moment and the determined average value plotted versus the theoretical d moment for different compounds. There is no direct correlation between the average value of the Fe CMXD and the theoretical p and d moments. A plot of the amplitude of the first maxima at $E=0$ eV or the minima at $E\sim 7$ eV gives no better correlation between the CMXD signal and the local moments.

But in the case of Co and Ni, obviously there exists a direct correlation between the average value of the μ_c/μ_0 signal and the p moment at the Ni and Co edges as seen from Fig. 9. In the case of Co, the calculation for Co metal, $Fe_{80}Co_{20}$, and the Pt/Co multilayered structures shows that an increase of the p moment seems to be correlated to an decrease of the d moment. The presented results may indicate that the Co CMXD could give direct information on the local magnetic Co moment. This finding is confirmed by the increase of the spin-dependent Co K absorption signal in Ce_2Co_{17}, for which a Co d moment of about $1.5\mu_B$ is estimated.[31] However, more systematic studies and theoretical calculations are planned to prove whether there exists a general relation of the CMXD signal at Co K edges and a local Co moment.

VI. SUMMARY

We presented systematic studies of spin-dependent K absorption measurements in 3d metals, binary alloys and compounds, and multilayered samples. The experimental data for Fe and Ni metals are well described by fully relativistic SP-KKR-GF calculations. In the case of the Ni and Co K edges, a direct correlation between the p moment and the average value of the μ_c/μ_0 signal can be found. But a comparison with the d moments shows that from the CMXD signal direct information on the local magnetic moments, which is predominantly carried by d electrons, might be deduced only in the case of Co. In the case of iron, no correlation between the CMXD signal and the local moment exists. But a comparison with spin-polarized band-structure calculations indicates that the spin-dependent absorption profile reflects the p-projected spin density of states and its changes in different chemical environments containing useful information on the magnetic aspects of the local electronic structures in metallic systems.

ACKNOWLEDGMENTS

We like to thank S. Welzel-Gerth for preparing the $Fe_{70}Pt_{30}$-Invar alloy and for experimental help, J. Hesse for the $Fe_{72.7}Pt_{27.3}$-Invar alloy, B. Scholz for the Fe/Tb multilayered structures, D. Weller for the $Pt_xMn_{1-x}Sb$ sample, G. Wiesinger for the Ho_6Fe_{23} compound, B. Zeper for preparing the Pt/Co multilayered structures, and P. Maier-Komor for the remaining samples. Useful discussions with E. Dartyge *et al.* and the help of the technical staff at the Technical University of Munich and HASYLAB at Hamburg are highly appreciated. This work is supported by BMFT Project No. 05 466 EAI.

[1]K. Namikawa, M. Ando, T. Nakajami, and H. Kawata, J. Phys. Soc. Jpn. **54**, 4099 (1985).

[2]G. van der Laan, B. T. Thole, G. A. Sawatzky, J. B. Goedkoop, J. C. Fuggle, J.-M. Esteva, R. Karnatak, J. P. Remeika, and H. A. Dabkowska, Phys. Rev. B **34**, 6529 (1986).

[3]G. Schütz, W. Wagner, W. Wilhelm, P. Kienle, R. Zeller, R. Frahm, and G. Materlik, Phys. Rev. Lett. **58**, 737 (1987).

[4]D. Gibbs, D. R. Harshman, E. D. Isaacs, D. B. McWhan, D. Mills, and C. Vettier, Phys. Rev. Lett. **61**, 1241 (1988).

[5]G. Schütz, R. Wienke, W. Wilhelm, W. Wagner, P. Kienle, R.

Zeller, and R. Frahm, Physica B **158**, 284 (1989).
[6]C. T. Chen, F. Sette, Y. Ma, and S. Modesty, Phys. Rev. B **42**, 7262 (1990).
[7]G. Schütz, M. Knülle, R. Wienke, W. Wilhelm, W. Wagner, P. Kienle, and R. Frahm, Z. Phys. B **73**, 67 (1988).
[8]G. Schütz, R. Wienke, W. Wilhelm, W. Wagner, P. Kienle, R. Zeller, and R. Frahm, Z. Phys. B **75**, 495 (1989).
[9]H. Ebert, H. Strange, and B. L. Gyorffy, Z. Phys. **73**, 77 (1988).
[10]D. Dräger, R. Frahm, G. Materlik, and O. Brümmer, Phys. Status. Solidi B **146**, 287 (1988).
[11]R. Wienke, G. Schütz, and H. Ebert, J. Appl. Phys. **69**, 6147 (1991).
[12]*Handbook on Synchrotron Radiation,* edited by E. E. Koch (North-Holland, Amsterdam, 1983), Vol. 1.
[13]*X-Ray Absorption,* edited by D. C. Koningsberger and R. Prins (Wiley, New York, 1988).
[14]U. Fano, Phys. Rev. Lett. **178**, 131 (1969).
[15]J. P. Desclaux, Comput. Phys. Commun. **1**, 216 (1969).
[16]H. C. Pauli and V. Raff, Comput. Phys. Commun. **9**, 392 (1975).
[17]P. J. Durham, *The Electronic Structure of Complex Systems,* edited by P. Phariseau and W. Temmerman (Plenum, New York, 1984), p. 709.
[18]P. Strange, H. Ebert, J. B. Staunton, and B. L. Gyorffy, J. Phys. Condens. Matter **1**, 2959 (1989).
[19]H. Ebert, G. Schütz, and W. M. Temmerman, Solid State Commun. **76**, 475 (1990).
[20]H. Ebert and H. Akai, in *Application of Multiple Scattering Theory to Materials Science,* edited by W. H. Butler, P. H. Dederichs, A. Gonis, and R. Weaver, Mater. Res. Soc. Symp. Proc. No. 253 (Materials Research Society, Pittsburgh, 1992), p. 329.
[21]J. E. Müller, O. Jepsen, and J. W. Wilkins, Solid State Commun. **42**, 365 (1982).
[22]The fcc Co was prepared by rapid quenching procedures.
[23]W. B. Zeper, F. Greidanus, P. Carcia, and C. Fincher, J. Appl. Phys. **65**, 4971 (1989).
[24]H. Sakurai (private communication).
[25]E. F. Wassermann, Adv. Solid State Phys. **27**, 85 (1987).
[26]*Physics and Applications of Invar Alloys,* Honda Memorial Series on Material Science No. 3 (Maruzen, Tokyo, 1978).
[27]K. Attenkofer *et al.* (unpublished).
[28]B. Scholz, R. A. Brand, W. Keune, U. Kirschbaum, E. F. Wassermann, K. Mibu, and T. Shinjo, J. Magn. Magn. Mater. **93**, 499 (1991).
[29]H. Ebert and G. Schütz, J. Appl. Phys. **69**, 4627 (1991).
[30]*Ferromagnetic Materials,* edited by E. P. Wohlfahrth (North-Holland, Amsterdam, 1980).
[31]The Co moments are estimated from the calculations of L. Nordström, O. Ericson, M. S. S. Brooks, and B. Johansson, Phys. Rev. B. **41**, 9111 (1990) and magnetization data of K. H. J. Buschow, Rep. Prog. Phys. **42**, 1373 (1979), taking into account the Ce 5*d* moments deduced from $L_{2,3}$ CMXD measurements of P. Fischer, G. Schütz, and S. Stähler, J. Appl. Phys. **69**, 6144 (1991).